

Phase sensitivity with a coherent beam and twin beams via intensity difference detection

Jun Liu(刘俊), Tao Shao(邵涛), Chenlu Li(李晨露), Minyang Zhang(张敏洋), Youyou Hu(胡友友), Dongxu Chen(陈东旭), and Dong Wei(卫栋)

Citation: Chin. Phys. B, 2024, 33 (**1**): 014203. DOI: 10.1088/1674-1056/ad0115
Journal homepage: http://cpb.iphy.ac.cn; http://iopscience.iop.org/cpb

What follows is a list of articles you may be interested in

Quantum-enhanced optical precision measurement assisted by low-frequency squeezed vacuum states

Guohui Kang(康国辉), Jinxia Feng(冯晋霞), Lin Cheng(程琳), Yuanji Li(李渊骥), and Kuanshou Zhang(张宽收)
Chin. Phys. B, 2023, 32 (**10**): 104204. DOI: 10.1088/1674-1056/acc520

Four-stage cascaded variable optical attenuator with large attenuation range for quantum key distribution

Qing-Hai Liu(刘清海), Pan Pan(潘盼), Jin You(游金), Jia-Shun Zhang(张家顺), Ya Wang(汪亚),Yu-Ting Wang(王玉婷), Liang-Liang Wang(王亮亮), Jun-Ming An(安俊明),Da-Jian Cui(崔大健), Lang Zhou(周浪), and Wei Chen(陈伟)
Chin. Phys. B, 2023, 32 (**5**): 054207. DOI: 10.1088/1674-1056/ac8af6

Quantum key distribution transmitter chip based on hybrid-integration of silica and lithium niobates

Xiao Li(李骁), Liang-Liang Wang(王亮亮), Jia-shun Zhang(张家顺), Wei Chen(陈巍), Yue Wang(王玥), Dan Wu (吴丹), and Jun-Ming An (安俊明)
Chin. Phys. B, 2022, 31 (**6**): 064212. DOI: 10.1088/1674-1056/ac40fe

Bright 547-dimensional Hilbert-space entangled resource in 28-pair modes biphoton frequency comb from a reconfigurable silicon microring resonator

Qilin Zheng(郑骑林), Jiacheng Liu(刘嘉成), Chao Wu(吴超), Shichuan Xue(薛诗川), Pingyu Zhu(朱枰谕), Yang Wang(王洋), Xinyao Yu(于馨瑶), Miaomiao Yu(余苗苗), Mingtang Deng(邓明堂), Junjie Wu(吴俊杰), and Ping Xu(徐平)
Chin. Phys. B, 2022, 31 (**2**): 024206. DOI: 10.1088/1674-1056/ac3507

Bandwidth-tunable silicon nitride microring resonators

Jiacheng Liu(刘嘉成), Chao Wu(吴超), Gongyu Xia(夏功榆), Qilin Zheng(郑骑林), Zhihong Zhu(朱志宏), and Ping Xu(徐平)
Chin. Phys. B, 2022, 31 (**1**): 014201. DOI: 10.1088/1674-1056/ac2e64

Phase sensitivity with a coherent beam and twin beams via intensity difference detection

Jun Liu(刘俊)[1,†], Tao Shao(邵涛)[1], Chenlu Li(李晨露)[1], Minyang Zhang(张敏洋)[1], Youyou Hu(胡友友)[1], Dongxu Chen(陈东旭)[2,‡], and Dong Wei(卫栋)[3]

[1] *School of Science, Jiangsu University of Science and Technology, Zhenjiang* 212003, *China*
[2] *Quantum Information Research Center, Shangrao Normal University, Shangrao* 334001, *China*
[3] *School of Physics, Xi'an Jiaotong University, Xi'an* 710049, *China*

(Received 10 July 2023; revised manuscript received 12 September 2023; accepted manuscript online 7 October 2023)

We focus on the Mach–Zehnder interferometer (MZI) with the input of a coherent beam and one of the bright entangled twin beams with an external power reference beam employed for measurement. The results show that the phase sensitivity can reach sub-Heisenberg limit and approach quantum Cramér–Rao bound by changing the squeezing parameters and the photon number of the coherent beam, under the phase-matching condition. The absence of the external power reference beam will degrade the performance of the phase sensitivity. Meanwhile, this scheme shows good robustness against the losses of the photon detectors. We present a detailed discussion about the phase sensitivities when the inputs are two coherent beams, or a coherent beam plus a single-mode squeezed vacuum beam based on the MZI. This scenario can be applied in the field of phase precision measurements and other optical sensors.

Keywords: Mach–Zehnder interferometer, phase sensitivity, quantum squeezing

PACS: 42.50.–p, 42.50.St, 03.65.Ta **DOI:** 10.1088/1674-1056/ad0115

1. Introduction

Interferometers play an important role in the field of precision measurement.[1–11] One of the most typical interferometers is the Mach–Zehnder interferometer (MZI). A general MZI is composed of two beam splitters (BS) and is used to measure phase shift variations in the two paths. The measurement sensitivity of such phase shifts can not surpass $1/\sqrt{N}$ when the inputs are the combination of a coherent state and an vacuum state, where N is the total photon number of the inputs, and $1/\sqrt{N}$ is named as the shot noise limit (SNL) or the standard quantum limit.[12]

In order to beat SNL, non-classical states such as the single-mode squeezed vacuum state and two-mode squeezed vacuum state are employed.[13–16] Then the phase sensitivity can reach $1/N$, which is also named as the Heisenberg limit (HL). When inputs are Fock state, N00N state and entangled coherent state, the phase sensitivity can also reach sub-SNL and HL.[3,17,18] However, there are many potential problems. For the N00N state, this input state has been shown to be very sensitive to losses, and the maximum photon number N remains very low in experiments.

Recently, due to the good performance in phase estimation, a coherent state and a single-mode squeezed vacuum state have been investigated by many groups.[10] Caves *et al.* claimed that when one of the inputs is a coherent state, the optimal state of the other input is the single-mode squeezed vacuum state,[15] which has been employed in LIGO.[16] When the inputs are the combination of a single-mode squeezed vacuum state and a coherent state, several detection methods are proposed, such as intensity detection, balanced homodyne detection and parity detection.[8] Different detection methods can lead to different optimal phase sensitivities. In order to achieve the optimal phase sensitivity, all the possible measurement strategies need to be taken into account, which is impossible. Fortunately, quantum Fisher information (QFI) and its related quantum Cramér–Rao bound (QCRB) are introduced to find the optimal theoretical phase sensitivity without considering the specific measurement strategies.

The QFI is an effective tool in the estimation process when the inputs are the coherent state, Fock state, single-mode squeezed vacuum state, and single-mode squeezed coherent state, etc.[19–28] However, with an external phase reference beam in the detection process, the QFI can be different, which is observed by Jarzyna *et al.*[19] In addition, Takeoka *et al.* used a phase-averaging method to solve this problem.[23] Later, You *et al.* claimed that the two-parameter phase estimation and the phase-averaging method is equivalent with specific inputs.[24] They also pointed out that it needs to take the reference beam into consideration when a phase reference beam is employed. Then, the detection strategy with external beams has aroused much concern.

Recently, squeezing and entanglement-assisted input states are proposed.[17,29–33] Under the condition of the squeezing-assisted input,[17,29] the intensity difference detec-

†Corresponding author. E-mail: junliu@just.edu.cn
‡Corresponding author. E-mail: chendx@sru.edu.cn

© 2024 Chinese Physical Society and IOP Publishing Ltd

tion with an external power reference beam is employed. In the detection process, the conjugate beam offers an external power reference and the phase sensitivity can reach sub-SNL. However, they only consider the condition that one of the inputs is the vacuum beam and the advantage of the external power reference beam is not shown. Meanwhile, the optimal phase sensitivity can only reach sub-SNL. In this paper, we focus on the phase sensitivity with one coherent beam plus one of the bright entangled twin beams (BETB). Moreover, we aim to show that when the inputs of the MZI are a coherent beam plus one of the BETB, the optimal phase sensitivity can reach sub-HL and approach QCRB.

This paper is structured as follows. In Section 2, the scheme with intensity difference detection is introduced. The QFI and the QCRB are introduced. In Section 3, we analyze how the phase sensitivity is affected by the factors. The impacts of the detection efficiencies of the photon detectors are also studied. Then, detailed comparisons are shown in Section 4. Finally, the conclusions are drawn in Section 5.

2. The proposed model and phase sensitivity estimation

2.1. The scheme and operator transformation

In the first part of Fig. 1, we show the generation process of the BETB, which is named as the two-mode squeezed process.[34–37] This two-mode squeezed process can be accomplished by the FWM experiments.[38–41] The FWM transformation can be expressed as

$$\begin{aligned}\hat{a}_1 &= \cosh r\hat{a}_0 + \sinh r\hat{b}_0^{\dagger}\mathrm{e}^{\mathrm{i}\theta_1},\\ \hat{b}_1 &= \mathrm{e}^{\mathrm{i}\theta_1}\sinh r\hat{a}_0^{\dagger} + \cosh r\hat{b}_0,\end{aligned} \tag{1}$$

where r is the parametric strength of the FWM, $\theta_1 = 2\theta_{\mathrm{pump}}$, and θ_{pump} is the phase of the pump beam; $\hat{a}_0$ ($\hat{a}_0^{\dagger}$) and $\hat{b}_0$ ($\hat{b}_0^{\dagger}$) are annihilation (creation) operators of the input modes of the FWM, respectively. We denote $\langle\hat{a}_0\rangle = |\alpha_a|\mathrm{e}^{\mathrm{i}\phi_a}$, with $|\alpha_a|$ and ϕ_a being the amplitude and phase of the coherent beam. The photon number N_{a0} is equal to $|\alpha_a|^2$. For the MZI, the intensities of the amplified probe beam and the generated conjugate beam are $\langle I_{\mathrm{p}}\rangle = \langle\hat{a}_1^{\dagger}\hat{a}_1\rangle = GN_{a0} + G - 1$ and $\langle I_{\mathrm{con}}\rangle = \langle\hat{b}_1^{\dagger}\hat{b}_1\rangle = (G-1)N_{a0} + G - 1$. Here, $G = \cosh^2 r$ and it is defined as gain; $\hat{a}_1$ ($\hat{a}_1^{\dagger}$), $\hat{b}_1$ ($\hat{b}_1^{\dagger}$) are the annihilation (creation) operators of the output modes of the FWM. Here, the BETBs mean the conjugate beam and the probe beam after FWM.

Next, a coherent beam and one of the BETBs enter the BS. For the BS, the input-output relationship can be shown as $\hat{a}_2 = \frac{1}{\sqrt{2}}\hat{a}_1 + \mathrm{i}\frac{1}{\sqrt{2}}\hat{c}_0$, and $\hat{c}_1 = \mathrm{i}\frac{1}{\sqrt{2}}\hat{a}_1 + \frac{1}{\sqrt{2}}\hat{c}_0$, which suggest that the transmissivity and reflectivity of the BS are $T = R = \frac{1}{2}$. Here $\hat{c}_0$ ($\hat{c}_0^{\dagger}$), $\hat{a}_2$ ($\hat{a}_2^{\dagger}$) and $\hat{c}_1$ ($\hat{c}_1^{\dagger}$) are annihilation and creation operators of the input-output modes of the first BS; $\langle\hat{c}_0\rangle = |\alpha_c|\mathrm{e}^{\mathrm{i}\phi_c}$, α_c and ϕ_c are amplitude and phase of the coherent beam. The photon number N_c is $|\alpha_c|^2$. The total transformation of the operators in the scenario is given by

$$\begin{aligned}\hat{a}_{\mathrm{out}} = &\frac{1}{2}(\mathrm{e}^{\mathrm{i}\phi} - 1)(\sqrt{G}\hat{a}_0 + \sqrt{G-1}\hat{b}_0^{\dagger}\mathrm{e}^{\mathrm{i}\theta_1})\\ &+ \frac{1}{2}(\mathrm{i}\,\mathrm{e}^{\mathrm{i}\phi} + \mathrm{i})\hat{c}_0,\end{aligned} \tag{2}$$

and the intensity after the MZI is $\langle\hat{I}_a\rangle = \langle\hat{a}_{\mathrm{out}}^{\dagger}\hat{a}_{\mathrm{out}}\rangle = \frac{1}{4}[m_1(GN_{a0} + G - 1) + 4\sin\phi\sqrt{G}\cos\phi_{\mathrm{d}}\sqrt{N_{a0}N_c} + m_2N_c]$, with the notations $m_1 = 2 - 2\cos\phi$ and $m_2 = 2 + 2\cos\phi$, $\phi_{\mathrm{d}} = \phi_a - \phi_c$. Note that, in the parts of input–output relationship and error propagation formula, we assume $\phi_1 = 0$ and $\phi_2 = \phi$. The intensity of the external power reference beam, $\langle\hat{I}_b\rangle$, is equal to $\langle I_{\mathrm{con}}\rangle$; $\hat{a}_{\mathrm{out}}$ ($\hat{a}_{\mathrm{out}}^{\dagger}$) is the annihilation (creation) operators of the mode after the second BS.

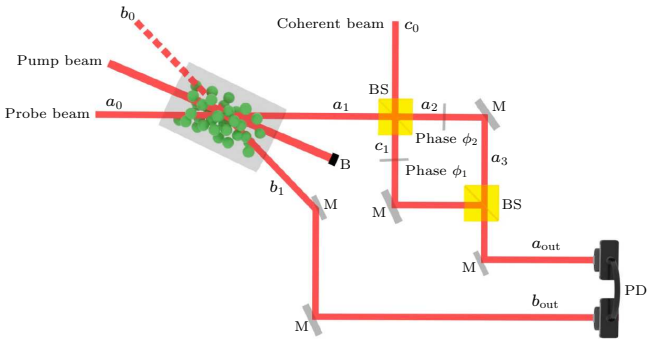


Fig. 1. The scheme for phase sensitivity measurement based on the Mach–Zehnder interferometer (MZI). For the MZI, the inputs are one of the bright entangled twin beams and one coherent beam. The intensity difference is employed for the measurement process. M: mirror; FWM: four-wave mixing; BS: beam splitter; PD: photon detector; B: beam block; dashed line: the vacuum beam.

2.2. Phase sensitivity estimation with intensity difference detection

According to the error propagation formula, the phase sensitivity $\Delta\phi$ as the uncertainty in estimating the phase shift ϕ is

$$\Delta\phi = \frac{\sqrt{\Delta^2\hat{I}_{-\mathrm{B}}}}{|(\partial_\phi\langle\hat{I}_{-\mathrm{B}}\rangle)|}. \tag{3}$$

The intensity difference detection signal can be expressed as $\langle\hat{I}_{-\mathrm{B}}\rangle = \langle\hat{a}_{\mathrm{out}}^{\dagger}\hat{a}_{\mathrm{out}} - \hat{b}_1^{\dagger}\hat{b}_1\rangle = \langle\hat{I}_a\rangle - \langle\hat{I}_b\rangle$. Then the slope can be expressed as

$$\begin{aligned}|(\partial_\phi\langle\hat{I}_{-\mathrm{B}}\rangle)| = \left|\frac{\partial\langle\hat{I}_{-\mathrm{B}}\rangle}{\partial\phi}\right| = \Big|&\frac{1}{2}\sin\phi(GN_{a0} + G - 1 - N_c)\\ &+ \cos\phi\cos\phi_{\mathrm{d}}\sqrt{G}\sqrt{N_{a0}N_c}\Big|,\end{aligned} \tag{4}$$

while the variance of intensity difference is

$$\begin{aligned}\Delta^2\hat{I}_{-\mathrm{B}} &= \langle\hat{I}_{-\mathrm{B}}^2\rangle - \langle\hat{I}_{-\mathrm{B}}\rangle^2\\ &= \left(\frac{m_2^2}{8}G^2 - \left(1 + \frac{\cos^2\phi}{2} + \frac{3\cos\phi}{2}\right)G + 1\right)N_{a0}\\ &\quad + \sin\phi\cos\phi_{\mathrm{d}}\sqrt{G}(1 + (\cos\phi + 1)(1 - G))\sqrt{N_{a0}N_c}\\ &\quad + \left(\frac{G\sin^2\phi}{2} + \frac{\cos\phi + \cos^2\phi}{2}\right)N_c\end{aligned}$$

$$+\left(\frac{Gm_2^2}{16}+\frac{\sin^2\phi}{4}\right)(G-1). \tag{5}$$

The photon number of the inputs is given by

$$N_{\rm B} = \langle I_{\rm p}\rangle + \langle I_c\rangle = GN_{a0}+G-1+N_c. \tag{6}$$

Therefore, the SNL and HL of the scenario in Fig. 1 is $1/\sqrt{N_{\rm B}}$ and $1/N_{\rm B}$.

2.3. The QFI and QCRB in two-parameter phase estimation

For the parameter estimation process, the QCRB is $(\Delta\phi)^2 \geq F(\phi)^{-1}$. The inputs in Fig. 1 are pure states. Under this constraint, the QFI $F(\phi)$ is

$$F(\phi) = 4{\rm Re}(\langle\partial_\phi\psi|\partial_\phi\psi\rangle - \langle\partial_\phi\psi|\psi\rangle\langle\psi|\partial_\phi\psi\rangle), \tag{7}$$

and $\partial_\phi\psi = \partial\psi/\partial\phi$, ψ is the state after the phase shift. In order to avoid the potential unavailable measurement strategy, two-parameter phase estimation is necessary. As shown in Fig. 1, there are two phases ϕ_1 and ϕ_2 in the two arms of the MZI, and we define the two-parameter QFI as

$$F = \begin{bmatrix} F_{jj} & F_{jk} \\ F_{kj} & F_{kk} \end{bmatrix}, \tag{8}$$

$$F_{jk} = 4{\rm Re}(\langle\partial_j\psi|\partial_k\psi\rangle - \langle\partial_j\psi|\psi\rangle\langle\psi|\partial_k\psi\rangle), \tag{9}$$

where $j,k\in(+,-)$. $F_{\rm jk}$ is the Fisher matrix element F. Re$(\cdot)$ means the real part. Here, $\phi_+ = (\phi_2+\phi_1)$ and $\phi_- = (\phi_2-\phi_1)$ mean sum and difference of the phases in the two arms of MZI; $\partial_j\psi = \partial\psi/\partial\phi_j$. The state after the phase shift can be displayed as $|\psi_{\rm out}\rangle = \hat{U}\hat{B}|\psi_{\rm in}\rangle$. $\hat{B}$ is the BS unitary transformation operator, and $\hat{U}$ mean the phase shift unitary operators. $\hat{B} = {\rm e}^{{\rm i}\hat{M}\pi/4}$ and $\hat{M} = \hat{a}_1^\dagger\hat{c}_0+\hat{c}_0^\dagger\hat{a}_1$. $\hat{U} = {\rm e}^{{\rm i}(\phi_2\hat{a}_2^\dagger\hat{a}_2+\phi_1\hat{c}_1^\dagger\hat{c}_1)} = {\rm e}^{{\rm i}\hat{N}_+\phi_+}{\rm e}^{{\rm i}\hat{N}_-\phi_-}$, $\hat{N}_+ = (\hat{a}_2^\dagger\hat{a}_2+\hat{c}_1^\dagger\hat{c}_1)/2$, $\hat{N}_- = (\hat{a}_2^\dagger\hat{a}_2-\hat{c}_1^\dagger\hat{c}_1)/2$; $|\psi_{\rm in}\rangle$ is the state before the first BS. Then

$$\begin{bmatrix} \Delta^2\phi_+ & \Delta\phi_+\Delta\phi_- \\ \Delta\phi_-\Delta\phi_+ & \Delta^2\phi_- \end{bmatrix} \geq \frac{1}{D_F}\begin{bmatrix} F_{--} & -F_{+-} \\ -F_{-+} & F_{++} \end{bmatrix}, \tag{10}$$

and $D_F = F_{--}F_{++}-F_{-+}F_{+-}$. We only focus on the phase difference ϕ_-. Therefore, $(\Delta^2\phi_-) \geq \frac{1}{F}$ and $F = F_{--}-\frac{F_{-+}F_{+-}}{F_{++}}$. The detailed expression is shown in Appendix A.

In Fig. 1, the inputs are one kind of two-mode squeezed state and a coherent state, which can be expressed as $|\psi_{\rm in}\rangle = \hat{D}_c\hat{S}(\xi)\hat{D}_a|0_a,0_c\rangle$, where $|0_a,0_c\rangle$ represents the vacuum state; $\hat{D}_a = {\rm e}^{\alpha_a\hat{a}^\dagger-\alpha_a^*\hat{a}}$ ($\hat{D}_c = {\rm e}^{\alpha_c\hat{c}^\dagger-\alpha_c^*\hat{c}}$) is the displacement operator with $\alpha_a = |\alpha_a|{\rm e}^{{\rm i}\phi_{\rm a}}$ ($\alpha_c = |\alpha_c|{\rm e}^{{\rm i}\phi_{\rm c}}$); $\hat{S}(\xi)$ is the two-mode squeezing operator which is defined as $\hat{S}(\xi) = {\rm e}^{\xi^*\hat{a}\hat{b}-\xi\hat{a}^\dagger\hat{b}^\dagger}$, where $\xi = r{\rm e}^{{\rm i}\theta_1}$, $\hat{a}$ ($\hat{a}^\dagger$) and $\hat{b}$ ($\hat{b}^\dagger$) are annihilation and creation operators of mode a (b), respectively. Substituting Eq. (1) into Eq. (10) yields

$$\begin{aligned} F_{--} &= N_B+2(G-1)N_c, \\ F_{-+} &= F_{+-} = -2G\sqrt{GN_{a0}N_c}\sin\phi_{\rm d}, \end{aligned}$$

$$F_{++} = G((2G-1)N_{a0}+G-1)+N_c. \tag{11}$$

The QCRB can be better with a larger F. Then the QFI F can be maximized with $F_{-+} = F_{+-} = 0$.

3. Analysis of the phase sensitivity

3.1. Results

According to Eqs. (3) and (11), figure 2 shows the phase sensitivity versus phase shift and phase difference with $r = 0.65$, $N_{a0} = 0.1$, and $N_c = 0.5$. The lower value $\Delta\phi$ represents the better phase sensitivity. In this scenario, with one of the BETB entering the MZI and the other one being employed for detection, the phase sensitivity can beat HL in Fig. 2(a), and the optimal phase sensitivity approaches the QCRB. In the inset of Fig. 2(a), it is apparent that the optimal phase sensitivity can approach QCRB. In Fig. 2(b), with the variation of the phase difference, the phase sensitivity can be optimal with $\phi_{\rm d} = k\pi$ (k is an integer). When $\phi_{\rm d} = k\pi+\pi/2$, both the QCRB and the optimal phase sensitivity with intensity difference detection become the worst. The optimal phase sensitivity with intensity difference detection can only approach the QCRB when $\phi_{\rm d} = k\pi$. Under this constraint, in the following part, we take $\phi_{\rm d} = 0$ for simplification.

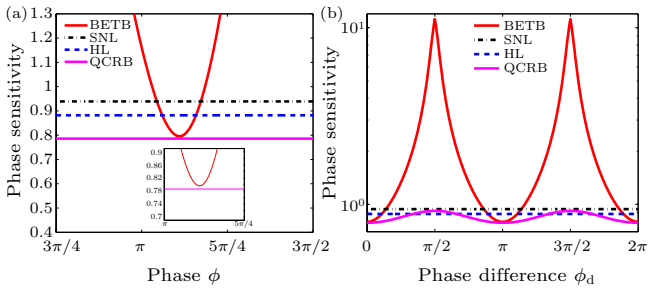


Fig. 2. Phase sensitivity versus phase shift (a) and phase difference (b). Others parameters are $r = 0.65$, $N_{a0} = 0.1$, and $N_c = 0.5$. In (a), $\phi_{\rm d} = 0$. BETB: bright entangled twin beams; SNL: shot noise limit; HL: Heisenberg limit; QCRB: quantum Cramér–Rao bound. The inset of (a) is the zoom of the phase sensitivity and it shows that the optimal phase sensitivity can not achieve the QCRB.

As shown in Fig. 3, the phase sensitivities vary with the squeezing parameter r, photon number N_{a0}, and N_c. When $N_{a0} = 0.1$ and $N_c = 0.5$, the phase sensitivity and the QCRB can beat HL with $r \leq 0.8$ in Fig. 3(a). When r increases, the phase sensitivity with intensity difference detection and the QCRB can only reach sub-HL. The optimal phase sensitivity always approaches QCRB with the increase of r. In Fig. 3(b), the optimal phase sensitivity and the QCRB beat HL when N_{a0} is less than 0.2. When N_{a0} becomes larger, they can reach sub-SNL. The optimal phase sensitivity approaches SNL when $N_{a0} \geq 1$. Figure 3(c) shows that both the optimal phase sensitivity and QCRB can reach sub-HL when $N_c \leq 0.9$. They become worse than HL when N_c becomes larger. In Fig. 3, only the photon number $N_{\rm B} \geq 1$ is considered.

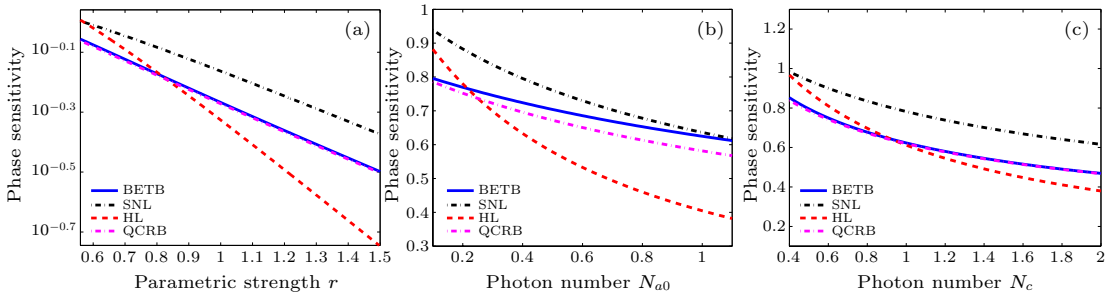


Fig. 3. Phase sensitivity versus parametric strength r (a), photon number N_{a0} (b), photon number N_c (c), with $r = 0.65$, $N_{a0} = 0.1$, and $N_c = 0.5$. The other parameters are the same as those in Fig. 2.

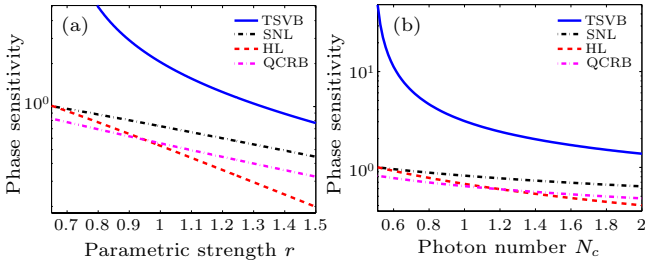


Fig. 4. Phase sensitivity versus parametric strength r (a) and photon number N_c (b). $N_{a0} = 0$. TSVB: two-mode squeezed vacuum beam. The other parameters are the same as those in Fig. 2.

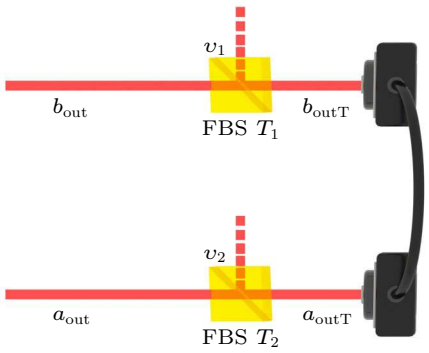


Fig. 5. The device for phase sensitivity measurement with transmissivity efficiencies T_1 and T_2 of the photon detectors. Fictitious beam splitters are employed to represent the losses of the photon detectors. The other parameters are the same as those in Fig. 2.

In the above subsections, we show the phase sensitivity with the inputs of a coherent beam and one of the BETB. In fact, when the photon number of the coherent beam N_c is zero, this scheme becomes the same as the scenario in Ref. [17]. If the squeezing parameter r is zero, for the MZI, the inputs are two coherent beams without the reference beam. With $N_{a0} = 0$, the inputs in Fig. 1 become a coherent beam and one of the two-mode squeezed vacuum beams (TSVB). The other one of the TSVB is employed as the external power reference beam. The phase sensitivities versus parametric strength r and photon number N_c are shown in Fig. 4. We immediately notice that the QCRB can beat HL and the optimal phase sensitivity with intensity difference detection is worse than SNL. In Fig. 4(a), the QCRB can only reach sub-SNL when r is more than 0.95 with $N_c = 0.5$. With $r = 0.65$, the QCRB can beat HL when $N_c \leq 1.1$ in Fig. 4(b). Therefore, for the input of a coherent beam plus one of TSVB based on the MZI, the intensity difference detection is not preferred.

3.2. Non-unit photon detection efficiency

In this subsection, we consider the condition that the detection efficiency of the photon detectors is not ideal in Fig. 5. Then the transformation of the operators in the scheme is expressed as

$$\begin{aligned} \hat{a}_{\text{outT}} &= \sqrt{T_2}\hat{a}_{\text{out}} + \sqrt{(1-T_2)}\hat{v}_2, \\ \hat{b}_{\text{outT}} &= \sqrt{T_1}\hat{b}_{\text{out}} + \sqrt{(1-T_1)}\hat{v}_1, \end{aligned} \tag{12}$$

where $\hat{v}_2$ ($\hat{v}_1$) and $\hat{a}_{\text{outT}}$ ($\hat{b}_{\text{outT}}$) are the annihilation operators of the two input-output modes of the fictitious BS, respectively. T_1 and T_2 represent the transmissivity of the detector. Only the losses of the photon detectors are considered and we assume that there are no losses inside the interferometer. The slope is given by

$$\left|\frac{\partial\langle\hat{I}_{-\text{BT}}\rangle}{\partial\phi}\right| = \left|T_2\frac{\partial\langle\hat{I}_{-\text{B}}\rangle}{\partial\phi}\right|, \tag{13}$$

and the variance of intensity difference is $\Delta^2\hat{I}_{-\text{BT}}$ (Details can be seen in Appendix B). As displayed in Fig. 6(a), with $T_2 = 0.2$ or 0.5, the phase sensitivity is always worse than SNL. With $T_2 = 0.8$, the phase sensitivity can beat SNL when T_1 is larger than 0.73. When the photon detector has no loss ($T_2 = 1$), the phase sensitivity is better than SNL with T_1 larger than 0.58. In this case, the better phase sensitivity can be achieved by the lower loss. According to Eq. (13), the transmissivity T_1 has no effects on the slope. The phase sensitivity is worse than SNL when the external power reference beam is absent ($T_1 = 0$). The external beam can boost the phase sensitivity by reducing the variance and keeping the slope unchanged. Note that the intensity difference detection will become intensity detection with $T_1 = 0$. The phase sensitivity can not beat SNL in this case. In Fig. 6(b), the larger the value T_2, the better the sensitivity. The phase sensitivity can beat SNL with T_2 larger than 0.76 with $T_1 = 0.8$. When $T_1 = 1$, the phase sensitivity can still reach SNL with $T_2 = 0.7$, which shows the good robustness of this scenario. In Fig. 6, with $r = 1$, $N_{a0} = 10$ and $N_c = 10^2$, the optimal phase sensitivity

with intensity difference detection can not surpass the HL with $T_1 = T_2 = 1$.

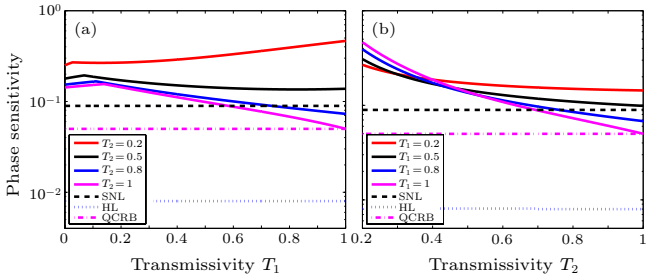


Fig. 6. Phase sensitivity with the increase of transmissivity T_1 (a) and T_2 (b), for $r = 1$, $N_{a0} = 10$, and $N_c = 10^2$. The other parameters are the same as those in Fig. 2.

4. Comparison

4.1. Two coherent beams with an external coherent beam

Next, another special scenario is considered. As shown in Fig. 7, two coherent beams enter the MZI, and another coherent beam is the external beam. Here, $\hat{a}_1$, $\hat{b}_1$ and $\hat{c}_0$ are annihilation operators of the input modes. N_{a2}, N_{b2} and N_{c2} are the photon numbers of the coherent beams. The intensities of the external coherent beam and the input coherent beam are the same as the intensities of the BETB in Fig. 1. Consequently, $N_{a2} = GN_{a0} + G - 1$, $N_{b2} = (G-1)N_{a0} + G - 1$, and $N_{c2} = N_c$. The SNL and HL in Figs. 1 and 7 are kept the same. The QFI $F_2 = N_{a2} + N_{c2} - \frac{4N_{a2}N_{c2}\sin^2\Delta\phi_{d2}}{N_{a2}+N_{c2}}$; $\phi_{d2} = \phi_{a2} - \phi_{c2}$; ϕ_{a2} and ϕ_{c2} are the phases of N_{a2} and N_{c2}. When $\phi_{\mathrm{d}2} = 0$, the QFI is maximal and QCRB $\Delta\phi$ can reach $\frac{1}{\sqrt{N_{a2}+N_{c2}}}$ (in this subsection, only $\phi_{d2} = 0$ is considered). With the error propagation formula, the slope yields

$$\left|\frac{\partial\langle\hat{I}_{-\mathrm{co}}\rangle}{\partial\phi}\right| = \left|\frac{1}{2}\sin\phi N_{a2} + \cos\phi\sqrt{N_{a2}N_{c2}} - \frac{1}{2}\sin\phi N_{c2}\right|, \quad (14)$$

and the variance becomes

$$\begin{aligned}\Delta^2\hat{I}_{-\mathrm{co}} &= \frac{1}{4}m_1N_{a2} + \sin\phi\sqrt{N_{a2}N_{c2}} + \frac{1}{4}m_2N_{c2} + N_{b2}\\ &= N_{\mathrm{co}} + N_{b2}. \end{aligned} \quad (15)$$

$N_{\mathrm{co}} = \frac{1}{4}m_1N_{a2} + \sin\phi\sqrt{N_{a2}N_{c2}} + \frac{1}{4}m_2N_{c2}$. We also impose $\phi_1 = 0$ and $\phi_2 = \phi$ in the error propagation formula. As displayed in Fig. 8, with the employment of the external beam, the QCRB can not surpass SNL. In Figs. 8(a) and 8(b), when the inputs are two coherent beams and another coherent beam is employed in the intensity difference detection, the phase sensitivity is worse than SNL. As displayed by Eqs. (14) and (15), when the external coherent beam is employed, the slope is unchanged and the variance becomes larger. Because $N_{\mathrm{co}} \geq 0$ and $N_{b2} \geq 0$, and $N_{\mathrm{co}} + N_{b2} \geq N_{\mathrm{co}}$. Hence the external coherent beam can not boost the phase sensitivity and makes it worse. As shown in Fig. 8(a), with the increase of N_{a0}, the photon number of the external coherent beam is larger and the phase sensitivities with the intensity difference detection can never approach SNL. Meanwhile, the QCRB can only reach SNL. In Fig. 8(b), the phase sensitivity with the intensity difference detection is worse than SNL with the increase of the photon number N_{c2}.

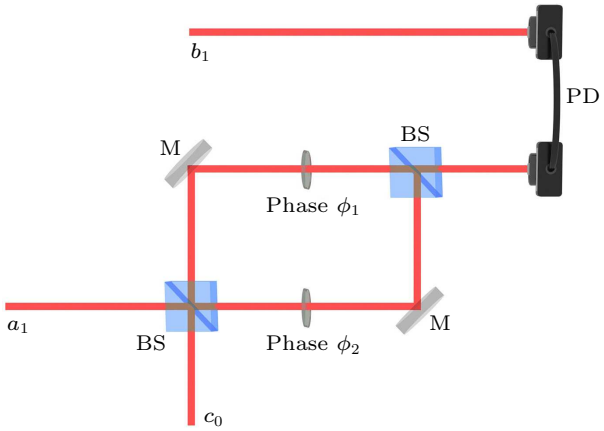


Fig. 7. The device for phase sensitivity measurement based on the Mach–Zehnder interferometer with two coherent beams and another coherent beam as the external beam. The other parameters are the same as those in Fig. 1.

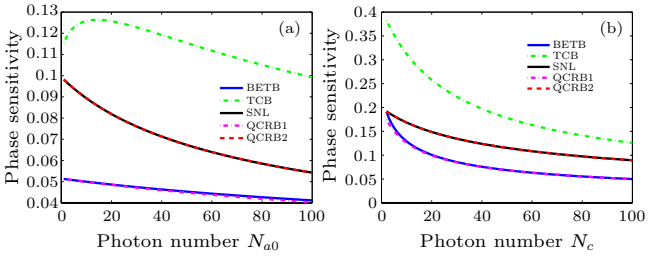


Fig. 8. Phase sensitivity versus parameter N_{a0} (a) and N_c (b), for $r = 1$, $N_{a0} = 10$, and $N_c = 10^2$. TCB means the phase sensitivity with two coherent beams and the intensity difference detection. The QCRB1 and QCRB2 are the quantum Cramér–Rao bounds with bright entangled twin beams and two coherent beams. The other parameters are the same as those in Fig. 2.

4.2. One coherent beam plus one single-mode squeezed vacuum beam

Next, the scheme in Fig. 1 is compared with that of the coherent beam plus single-mode squeezed vacuum beam scenario, which has an importance in LIGO.[16] The generation process of the single-mode squeezed vacuum beam can be described by the single-mode squeezed process, which is $\hat{S}_3(\xi_3)|0\rangle$. Here $|0\rangle$ means the vacuum state and $\hat{S}_3(\xi_3)$ is the single-mode squeezing operator. $\hat{S}_3(\xi_3) = \mathrm{e}^{[\xi_3^*(\hat{a})^2 - \xi_3(\hat{a}^\dagger)^2]/2}$, and $\xi_3 = r_3\mathrm{e}^{\mathrm{i}\phi_3}$, r_3 and ϕ_3 are the squeezing parameter strength and phase of the single-mode squeezing operator. In the coherent beam plus single-mode squeezed vacuum beam input scenario, the QCRB can reach $1/\sqrt{N_{c3}\mathrm{e}^{2r_3} + \sinh^2 r_3}$ and the optimal phase sensitivity is $1/\sqrt{N_{c3}\mathrm{e}^{2r_3}}$. N_{c3} is the photon number of the coherent beam. The photon number inside the MZI is $N_{c3} + \sinh^2 r_3$. The phase sensitivity can reach HL when $N_{c3} \simeq \sinh^2 r_3 \simeq \bar{n}_3/2$. Meanwhile, the maximum value of the squeezing degree r_3 can reach 1.7 (15.3 dB) in

Ref. [42]. In this case, the QCRB and the optimal phase sensitivity can reach HL, respectively. Considering the phase insensitive intensity squeezing degree being less than 10 dB, G is below 5.5 ($r \leq 1.5$).

As shown in Figs. 9(a) and 9(b), with $N_{c3} = \sinh^2 r_3$, the QCRB of the coherent beam plus the single-mode squeezed vacuum beam can surpass HL. With $r_3 = 0.8$, the QCRB of the coherent beam plus the BETB can beat HL. However, they are still worse than that of the coherent beam plus a single-mode squeezed vacuum beam. Note that the two scenarios have the same photon numbers N_B and the BETB have been the TSVB with $N_c = 0$. In Figs. 9(c) and 9(d), the practical experiments conditions $N_{c3} \gg \sinh^2 r_3$ are considered. In this case, both the QCRBs of the Fig. 1 and the coherent beam plus the single-mode squeezed vacuum state scenario can only reach sub-SNL. However, with the increase of the squeezing parameter r ($r > 1.86$), the QCRB with BETB can beat QCRB of the coherent beam plus a single-mode squeezed vacuum beam in Fig. 9(c). In Fig. 9(d), the BETB have become the TSVB, and the QCRB1 can still beat the QCRB2 ($r > 1.8$). According to Fig. 9, in the HL scale, the QCRB of the scenario in Fig. 1 is worse than that of the coherent beam plus a single-mode squeezed vacuum beam. However, in the sub-SNL region, with the high squeezing parameter r, the QCRB1 can beat the QCRB2. Though the squeezing parameter cannot be experimentally realized at present, it is hopeful that it can be achieved in the future.

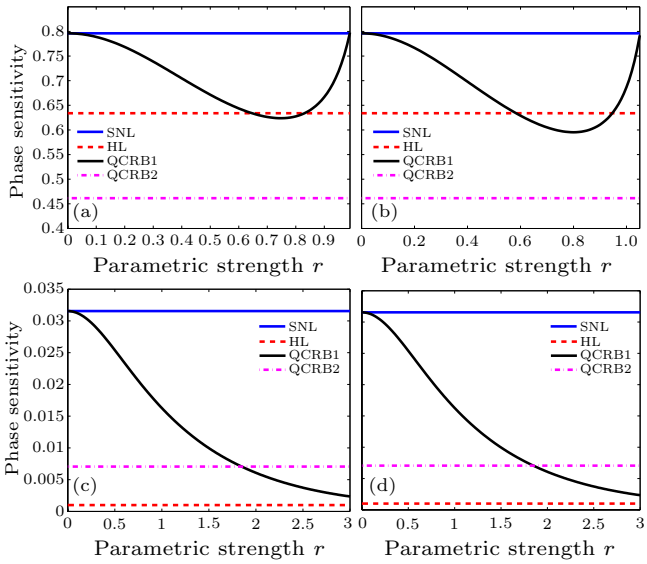


Fig. 9. Phase sensitivity versus parameter r. In (a) and (b), $r_3 = 0.8$, and in (c) and (d) $r_3 = 1.5$. $N_{a0} = 0.1$ in (a) and (c). In (b) and (d), $N_{a0} = 0$. $N_{c3} = \sinh^2 r_3$ in (a) and (b). $N_{c3} + \sinh^2 r_3 = N_B$, and they have the same SNL and HL. QCRB1 and QCRB2 are the quantum Cramér–Rao bounds of Fig. 1 and the scenario with the input of a coherent beam plus a single-mode squeezed vacuum beam. The other parameters are the same as those in Fig. 2.

5. Conclusion

In conclusion, this paper presents the phase sensitivity with the inputs of the BETB and coherent beams based on the MZI. The optimal phase sensitivity with intensity difference detection can reach sub-HL and approach QCRB while an external power reference beam is employed. When the inputs are a coherent beam plus one of the TSVB, the QCRB can beat HL and the optimal phase sensitivity with the intensity difference detection is worse than the SNL. We have a detailed discussion about the detection efficiencies of the photon detectors. The results show that the external beam play a vital role in the measurement process and the absence of the external beam can degrade the performance of the phase sensitivity dramatically. The QCRB of the scheme can be better than that of the coherent beam plus a single-mode squeezed vacuum beam input scenario with the high squeezing parameter. Meanwhile, the external coherent beam can not boost the phase sensitivity when the inputs are two coherent beams. This method of employing the external power reference beam offers a novel measurement way for the phase precision measurement.

Appendix A: Exact expression of the QFI elements

The QFI matrix elements can be expressed as

$$\begin{aligned}
F_{--} =& \mathrm{Re}[-\langle \hat{a}_1^\dagger \hat{c}_0 \hat{a}_1^\dagger \hat{c}_0\rangle + \langle \hat{a}_1^\dagger \hat{c}_0 \hat{a}_1 \hat{c}_0^\dagger\rangle + \langle \hat{a}_1 \hat{c}_0^\dagger \hat{a}_1^\dagger \hat{c}_0\rangle \\
& - \langle \hat{a}_1 \hat{c}_0^\dagger \hat{a}_1 \hat{c}_0^\dagger\rangle + \langle \hat{a}_1^\dagger \hat{c}_0\rangle^2 + \langle \hat{a}_1 \hat{c}_0^\dagger\rangle^2 - 2\langle \hat{a}_1^\dagger \hat{c}_0\rangle\langle \hat{a}_1 \hat{c}_0^\dagger\rangle], \\
F_{-+} =& \mathrm{Im}[\langle \hat{a}_1^\dagger \hat{c}_0 \hat{a}_1^\dagger \hat{a}_1\rangle + \langle \hat{a}_1^\dagger \hat{c}_0 \hat{c}_0^\dagger \hat{c}_0\rangle - \langle \hat{a}_1 \hat{c}_0^\dagger \hat{a}_1^\dagger \hat{a}_1\rangle - \langle \hat{a}_1 \hat{c}_0^\dagger \hat{c}_0^\dagger \hat{c}_0\rangle \\
& - \langle \hat{a}_1^\dagger \hat{c}_0\rangle\langle \hat{a}_1^\dagger \hat{a}_1\rangle - \langle \hat{a}_1^\dagger \hat{c}_0\rangle\langle \hat{c}_0^\dagger \hat{c}_0\rangle + \langle \hat{a}_1 \hat{c}_0^\dagger\rangle\langle \hat{a}_1^\dagger \hat{a}_1\rangle \\
& + \langle \hat{a}_1 \hat{c}_0^\dagger\rangle\langle \hat{c}_0^\dagger \hat{c}_0\rangle], \\
F_{+-} =& \mathrm{Im}[\langle \hat{a}_1^\dagger \hat{a}_1 \hat{a}_1^\dagger \hat{c}_0\rangle + \langle \hat{c}_0^\dagger \hat{c}_0 \hat{a}_1^\dagger \hat{c}_0\rangle - \langle \hat{a}_1^\dagger \hat{a}_1 \hat{a}_1 \hat{c}_0^\dagger\rangle - \langle \hat{c}_0^\dagger \hat{c}_0 \hat{a}_1 \hat{c}_0^\dagger\rangle \\
& - \langle \hat{a}_1^\dagger \hat{a}_1\rangle\langle \hat{a}_1^\dagger \hat{c}_0\rangle - \langle \hat{c}_0^\dagger \hat{c}_0\rangle\langle \hat{a}_1^\dagger \hat{c}_0\rangle + \langle \hat{a}_1^\dagger \hat{a}_1\rangle\langle \hat{a}_1 \hat{c}_0^\dagger\rangle \\
& + \langle \hat{c}_0^\dagger \hat{c}_0\rangle\langle \hat{a}_1 \hat{c}_0^\dagger\rangle], \\
F_{++} =& \mathrm{Re}[\langle \hat{a}_1^\dagger \hat{a}_1 \hat{a}_1^\dagger \hat{a}_1\rangle + \langle \hat{a}_1^\dagger \hat{a}_1 \hat{c}_0^\dagger \hat{c}_0\rangle + \langle \hat{c}_0^\dagger \hat{c}_0 \hat{a}_1^\dagger \hat{a}_1\rangle + \langle \hat{c}_0^\dagger \hat{c}_0 \hat{c}_0^\dagger \hat{c}_0\rangle \\
& - \langle \hat{a}_1^\dagger \hat{a}_1\rangle\langle \hat{a}_1^\dagger \hat{a}_1\rangle - 2\langle \hat{a}_1^\dagger \hat{a}_1\rangle\langle \hat{c}_0^\dagger \hat{c}_0\rangle - \langle \hat{c}_0^\dagger \hat{c}_0\rangle\langle \hat{c}_0^\dagger \hat{c}_0\rangle].
\end{aligned} \tag{A1}$$

$\mathrm{Im}(\cdot)$ represents the imaginary part.

Appendix B: Slope and variance of intensity difference with non-unit photon detection efficiency

The slope is given by

$$\begin{aligned}
\left|\frac{\partial\langle \hat{I}_{-\mathrm{BT}}\rangle}{\partial\phi}\right| =& \left|\frac{1}{2}T_2 \sin\phi (GN_{a0} + G - 1 - N_c)\right. \\
& \left. + T_2 \cos\phi \sqrt{G}\sqrt{N_{a0}N_c}\right|,
\end{aligned} \tag{B1}$$

and the variance of intensity difference $\Delta^2 \hat{I}_{-\mathrm{BT}}$ yields

$$\begin{aligned}
\Delta^2 \hat{I}_{-\mathrm{BT}} =& |\langle \hat{I}^2_{-\mathrm{BT}}\rangle - \langle \hat{I}_{-\mathrm{BT}}\rangle^2| \\
=& \left(\frac{1}{4}T_2 m_1 G - T_1(G-1)\right)^2 N_{a0} \\
& + \frac{1}{4}T_2^2 \sin^2\phi G(N_{a0} + N_c) + \frac{1}{16}T_2^2 m_2^2 N_c
\end{aligned}$$

$$
\begin{aligned}
&+G(G-1)\left(\frac{1}{4}T_2m_1-T_1\right)^2(N_{a0}+1)\\
&+\frac{1}{4}T_2^2\sin^2\phi(G-1)(N_c+1)\\
&+T_2\sin\phi\sqrt{G}\left[(G-1)\left(\frac{1}{4}T_2m_1-2T_1\right)\right.\\
&\left.+\frac{1}{4}T_2m_1G+\frac{1}{4}T_2m_2\right]\sqrt{N_{a0}N_c}\\
&+\frac{1}{4}T_2(1-T_2)(4\sin\phi\sqrt{GN_cN_{a0}}\\
&+m_2N_c+m_1(GN_{a0}+G-1))\\
&+T_1(1-T_1)(G-1)(N_{a0}+1). \qquad \text{(B2)}
\end{aligned}
$$

In this part, for simplification, we assume that $\phi_{\rm d}=0$.

Acknowledgments

Project supported by the National Natural Science Foundation of China (Grant Nos. 12104190, 12104189, and 12204312), the Natural Science Foundation of Jiangsu Province (Grant No. BK20210874), the Jiangsu Provincial Key Research and Development Program (Grant No. BE2022143); the Jiangxi Provincial Natural Science Foundation (Grant Nos. 20224BAB211014 and 20232BAB201042), and the General Project of Natural Science Research in Colleges and Universities of Jiangsu Province (Grant No. 20KJB140008).

References

[1] Scully M O and Zubairy M S 1997 *Quantum Optics* (Cambridge: Cambridge University Press)
[2] Braunstein S L and Loock P v 2005 *Rev. Mod. Phys.* **77** 513
[3] Caves C M 1981 *Phys. Rev. D* **23** 1693
[4] Boto A N, Kok P, Abrams D S, Braunstein S L, Williams C P and Dowling J P 2000 *Phys. Rev. Lett.* **85** 2733
[5] Xiao M, Wu L A and Kimble H J 1987 *Phys. Rev. Lett.* **59** 278
[6] Hou L L, Wang S and Xu X F 2020 *Chin. Phys. B* **29** 034203
[7] Sparaciari C, Olivares S and Paris M G A 2016 *Phys. Rev. A* **93** 023810
[8] Ataman S 2019 *Phys. Rev. A* **100** 063821
[9] Ataman S, Preda A and Ionicioiu R 2018 *Phys. Rev. A* **98** 043856
[10] Pezze L and Smerzi A 2008 *Phys. Rev. Lett.* **100** 073601
[11] Ono T and Hofmann H F 2010 *Phys. Rev. A* **81** 033819
[12] Sahota J and Quesada N 2015 *Phys. Rev. A* **91** 013808
[13] Anisimov P M, Raterman G M, Chiruvelli A, Plick W N, Huver S D, Lee H and Dowling J P 2010 *Phys. Rev. Lett.* **104** 103602
[14] Dowling J P 2008 *Contem. Phys.* **49** 125
[15] Lang M D and Caves C M 2013 *Phys. Rev. Lett.* **111** 173601
[16] Goda K, Miyakawa O, Mikhailov E E, Saraf S, Adhikari R, Mckenzie K, Ward R, Vass S, Weinstein A J and Mavalvala N 2008 *Nat. Phys.* **4** 472
[17] Liu J, Yu Y, Wang C Y, Chen Y, Wang J, Chen H, Wei D, Gao H and Li F 2020 *New J. Phys.* **22** 013031
[18] Pezze L and Smerzi A 2013 *Phys. Rev. Lett.* **110** 163604
[19] Jarzyna M and Demkowicz-Dobrzanski R 2012 *Phys. Rev. A* **85** 011801(R)
[20] Frowis F, Sekatski P and Dur W 2016 *Phys. Rev. Lett.* **116** 090801
[21] Zhang Y M, Li X W, Yang W and Jin G R 2013 *Phys. Rev. A* **88** 043832
[22] Liu J, Jing X X and Wang, X G 2013 *Phys. Rev. A* **88** 042316
[23] Takeoka M, Seshadreesan K P, You C L, Izumi S and Dowling J P 2017 *Phys. Rev. A* **96** 052118
[24] You C, Adhikari S, Ma X, Sasaki M, Takeoka M and Dowling J P 2019 *Phys. Rev. A* **99** 042122
[25] Gard B, You C, Mishr D, Singh R, Lee H, Corbitt T and Dowling J P 2017 *EPJ Quantum Technol.* **4** 4
[26] Zhong W, Wang F, Zhou L, Xu P and Sheng Y B 2020 *Sci. China Phys. Mech. Astron.* **63** 260312
[27] Ataman S 2022 *Phys. Rev. A* **105** 012604
[28] Zhang J and Wang S 2023 *Phys. Rev. A* **107** 043704
[29] Liu J, Wang Y X, Zhang M, Wang J, Wei D and Gao H 2020 *Opt. Express* **28** 39443
[30] Huang Z, Macchiavello C and Maccone L 2016 *Phys. Rev. A* **94** 012101
[31] Wang K, Wang X, Zhan X, Bian Z, Li J, Sanders B and Xue P 2018 *Phys. Rev. A* **97** 042112
[32] Zhang J and Wang S 2022 *Optik* **271** 170171
[33] Davis A, Sorelli G, Thiel V and Smith B 2022 *Phys. Rev. A* **105** 022601
[34] Boyer V, Marino A M and Lett P D 2008 *Phys. Rev. Lett.* **100** 143601
[35] Liu J, Wei D, Wang J W, Yu Y, Hu H J, Gao H and Li F L 2016 *Chin. Phys. B* **25** 114204
[36] Embrey C S, Turnbull M T, Petrov P G and Boyer V 2015 *Phys. Rev. X* **5** 031004
[37] Fang Y and Jing J 2015 *New J. Phys.* **17** 023027
[38] Jing J, Liu C, Zhou Z, Ou Z and Zhang W 2011 *Appl. Phys. Lett.* **99** 011110
[39] Zhang J, Jin C, Zhang Z, Cen L, Hu J and Zhao Y 2018 *Opt. Express* **26** 33080
[40] Plick W N, Dowling J P and Agarwal G S 2010 *New J. Phys.* **12** 083014
[41] Anderson B E, Schmittberger B L, Gupta P, Jones K M and Lett P D 2017 *Phys. Rev. A***95** 063843
[42] Vahlbruch H, Mehmet M, Danzmann K and Schnabel R 2016 *Phys. Rev. Lett.* **117** 110801